PLANT SCIENCE TODAY
ISSN 2348-1900 (online)
Vol 11(4): 373-384
https://doi.org/10.14719/pst.2922

HORIZON
e-Publishing Group
HePG

RESEARCH ARTICLE

In silico molecular docking, antimicrobial and anti-inflammatory activities of bioactive fractions of *Citrus sinensis* (L.) Osbeck. peel against oral pathogens in dental caries

Satyaprakash Dehury[1], Priyanka Priyadarsini[1], Ashirbad Nanda[1], Debasmita Dubey[2], Sandeep Kumar Swain[3], Biswajit Samantaray[4], Barsha Tripathy[5] & Satish Kanhar[1*]

[1]School of Pharmacy and Life Sciences, Centurion University of Technology and Management, Odisha, India
[2]IMS & Sum Hospital Medical College, Siksha O Anusandhan University, Bhubaneswar, Odisha, India
[3]ICMR-National Institute of Pathology, Advanced Molecular Diagnostic Lab Facilities, New Delhi, India
[4]School of Pharmaceutical Sciences, Siksha O Anusandhan University, Bhubaneswar, Odisha, India
[5]Department of Vegetable Sciences, Siksha O Anusandhan University, Bhubaneswar, Odisha, India

*Email: satishkanhar4@gmail.com

OPEN ACCESS

ARTICLE HISTORY

Received: 26 September 2023
Accepted: 05 March 2024

Available online
Version 1.0 : 31 March 2024
Version 2.0 : 01 October 2024

Check for updates

Additional information

Peer review: Publisher thanks Sectional Editor and the other anonymous reviewers for their contribution to the peer review of this work.

Reprints & permissions information is available at https://horizonepublishing.com/journals/index.php/PST/open_access_policy

Publisher's Note: Horizon e-Publishing Group remains neutral with regard to jurisdictional claims in published maps and institutional affiliations.

Indexing: Plant Science Today, published by Horizon e-Publishing Group, is covered by Scopus, Web of Science, BIOSIS Previews, Clarivate Analytics, NAAS, UGC Care, etc
See https://horizonepublishing.com/journals/index.php/PST/indexing_abstracting

CITE THIS ARTICLE

Dehury S, Priyadarsini P, Nanda A, Dubey D, Swain S K, Samantaray B, Tripathy B, Kanhar S. *In silico* molecular docking, antimicrobial and anti-inflammatory activities of bioactive fractions of *Citrus sinensis* (L.) Osbeck. peel against oral pathogens in dental caries. Plant Science Today. 2024; 11(4): 373-384. https://doi.org/10.14719/pst.2922

Abstract

Dental caries is the most prevalent oral disease. It is caused by infection of *Streptococcus mutans* and *Candida albicans*. It is associated with inflammation of the dental gum. Antimicrobial agents or systemic antibiotics are administered to prevent dental caries. However, the pathogens become drug-resistant to specific antibiotics, so a combinational therapy approach may lead to the management of dental caries. In the current investigation, the peel of *Citrus sinensis* (L.) Osbeck was evaluated for antimicrobial and anti-inflammatory activities in dental caries. Different fractions of hydroalcohol extract were tested for *in vitro* antimicrobial activity against *S. mutans* and *C. albicans*. Based on the results, methanol fraction was selected for *ex-vivo* anti-inflammatory activities. The bioactive compounds of the methanol faction were identified by GC-MS. Only selected compounds were subjected to *in silico* docking analysis towards selective proteins of *S. mutans* and *C. albicans*. Amongst all the fractions, the methanol fraction showed significant antimicrobial activity against *S. mutans* (ZOI, 27 mm; MIC, 0.78 mg/ml; and MBC, 1.56 mg/ml) and *C. albicans* (ZOI, 29 mm; MIC, 0.39 mg/ml; and MBC, 1.56 mg/ml). Methanol fraction (100 µg/ml) exhibited the highest inhibition of 79.29% than other fractions in the anti-inflammatory study. GC-MS analysis of methanol fraction reported 17 compounds. Out of these, only ten compounds satisfied Lipinski's rule of five in ADMET analysis and were subjected to *in silico* docking analysis. The results confirmed that the compounds of methanol fraction have the potential to inhibit the active proteins of dental caries pathogen.

Keywords

Citrus sinensis; *Streptococcus mutans*; *Candida albicans*; inflammation; GC-MS analysis

Introduction

Antimicrobial resistance poses a formidable challenge to global healthcare, with infectious agents such as bacteria, parasites, viruses, and fungi exhibiting resilience to conventional antibiotics. Recent publications from the United Kingdom government project that, by 2050, an alarming 10 million individuals annually will succumb to infections caused by antimicrobial-resistant pathogens (1). The intricate microbial landscape of the oral cavity, harboring approximately 700-1000 distinct microorganisms, is implicated in the onset of oral ailments, including periodontal disease

and dental caries (2). Furthermore, these oral pathogens can traverse the oral mucosa, entering systemic circulation and elevating antibody levels, contributing to the development of cardiovascular diseases (3). Evidently, oral biofilm-forming pathogens have demonstrated genetic or phenotypic resistance to existing antibiotic regimens (4). In the contemporary medical landscape, traditional herbal medicine has gained widespread acceptance globally. The World Health Organization (WHO) ensures rigorous standards for the quality and safety of herbal drugs employed in diverse therapeutic applications. Consequently, researchers are actively exploring novel chemical entities derived from plant sources, adhering to stringent regulatory criteria, as potential remedies to counteract the escalating threat posed by life-threatening pathogens.

Citrus sinensis, a member of the Rutaceae family, is a prominent fruit widely cultivated in India, serving as a significant nutritional source. Traditional applications involve its utilization in addressing diverse ailments, including diarrhea, constipation, respiratory conditions (cough, cold, bronchitis, tuberculosis), metabolic disorders (obesity, hypertension, angina), menstrual irregularities, and psychological concerns (depression, anxiety, stress). The therapeutic attributes of this fruit are ascribed to its rich content of vitamins B1, B2, B3, B5, B6, and vitamin C, alongside various minerals like calcium, iron, zinc, magnesium, and potassium (5). Pharmacological investigations support its antibacterial efficacy against *Escherichia coli, Pseudomonas aeruginosa, Staphylococcus aureus, Bacillus subtilis,* and Shigella, with petroleum ether, ethanol, and aqueous extracts displaying effectiveness against *C. albicans* (6-8). Notably, different extracts (hexane, chloroform, ethyl acetate, methanol, acetone) from C. *sinensis* peel exhibit moderate antiparasitic activity against *Plasmodium flacifarum* (9). Furthermore, the fruit demonstrates considerable antioxidant, antiproliferative, hypocholesterolemic, antiobesity, antiosteoprotic, and insecticidal properties (10). This study focuses on *in vitro* antimicrobial assessment of various solvent fractions from C. *sinensis* peel against multidrug-resistant dental caries pathogens. Recognizing the association between dental caries and gingival inflammation, an ex-vivo anti-inflammatory assay was conducted. Additionally, bioactive secondary metabolites from potent fractions were identified using GC-MS analysis. Their inhibitory potential against microbial proteins implicated in dental caries progression was established through an *in silico* analysis method.

Materials and Methods

Collection and preparation of extract

Citrus sinensis specimens were procured from a local market in Odisha, India, and subsequently authenticated by Dr. Gyanranjan Mahalik, Associate Professor in the Department of Botany at Centurion University of Technology and Management. A voucher specimen (voucher no. CUTM/BOT/2022/029) was meticulously cataloged and deposited in the herbarium of Centurion University of Technology and Management in Bhubaneswar, Odisha, serving as a reference for future research endeavors. The peels, have been meticulously collected, underwent a process of thorough cleansing with distilled water before undergoing a four-day shade-drying period. Following the drying phase, the peels were ground into a fine powder to facilitate extraction. A mass of 200 grams of the powdered material was subjected to a hydroalcoholic solution (ethanol: water, 70:30 v/v) in a percolator for a duration of 24 hours, with periodic stirring. This extraction process was repeated thrice over a span of 72 hours, and the resulting filtrate was collected. Subsequently, the hydroalcoholic extract underwent fractionalization employing petroleum ether, chloroform, ethyl acetate, acetone, and methanol to yield distinct fractions. Each fraction was subjected to evaporation in a rotary evaporator under reduced pressure, resulting in a semi-solid mass. This product was then stored in a desiccator for subsequent utilization (11).

Sample collection, isolation, and identification of microorganisms

Antimicrobial study of *C. sinensis*

Specimens were meticulously collected aseptically from dental patients at IMS, SUM Hospital, India, with explicit patient consent. Prior to dental caries sample collection, patients were instructed to rinse the tooth with water, followed by isolation with a rubber dam. Subsequently, the tooth underwent decontamination using 3% hydrogen peroxide and 2.5% sodium hypochlorite. Removal of food debris from the chewing surface was performed using a dental excavation instrument. Aseptically, a physician obtained the dental caries sample, placing it in 2 ml TGB or BHI broth in sterile screw cap bottles. Following thorough mixing with a magnetic stirrer, the samples were inoculated onto Muller Hinton broth (MHB) using the streak plate technique and incubated at 37 °C for 18 h. Post-incubation, samples were observed and sub-cultured in fresh MHB and Sabouraud dextrose agar (SDA) until obtaining pure cultures of bacteria and fungi. Identification of microorganisms was achieved through morphological, microscopic, and biochemical tests (12-13).

Evaluation of antimicrobial activity

Sterilized media aliquots were dispensed into petri plates and solidified. Bacterial and fungal suspensions were inoculated on Mueller-Hinton agar (MHA) and Sabouraud Dextrose Agar (SDA), respectively. Wells with a 6 mm diameter were created, and 100 µl aliquots (5 mg/ml) of various solvent fractions (petroleum ether, chloroform, ethyl acetate, acetone, and methanol) diluted with 10% DMSO were added. Gentamicin (100 µl, 30 mg/ml) and amphotericin B (100 µl, 10 mg/ml) served as standard drug controls for bacteria and fungi. Incubation was carried out at 37±2 °C for 24 h and 30±2 °C for 72 h for bacteria and fungi, respectively. The experiment was conducted in triplicate, and the inhibition zones were measured in

millimeters (12, 14).

Determinations of minimum inhibitory (MIC), minimum bactericidal concentration (MBC), and minimum fungicidal concentration (MFC)

The microdilution method was employed to conduct MIC, MBC, and MFC studies on bioactive fractions, specifically acetone and methanol fractions. Various concentrations (0.1–6.5 mg/ml) were prepared in 10% DMSO, and 100 µl of each fraction was added to a 96-well microplate containing an aliquot of the test sample, Muller-Hinton broth (100 µl), and bacterial or fungal inoculum (20 µl, 10^9 CFU/ml). Additionally, 5% 2,3,5-triphenyl tetrazolium chloride (TTC) dye (5 µl) was included in each well. Incubation occurred at 37 °C for 18 h (bacteria) and 48 h (fungi). MIC determination involved observing microbial growth. MBC and MFC were determined by incubating MIC samples at 37±2 °C for 24 h (bacteria) and 30±2 °C for 72 h (fungi). The minimum sample concentration exhibiting no growth was considered the MBC/MFC (12, 14).

Ex-vivo anti-inflammatory assay

A study investigating the anti-inflammatory effects on red blood cell (RBC) in healthy human volunteers was conducted. Blood samples were obtained and treated with an anticoagulant solution (Alsever's solution), followed by centrifugation at 3000 rpm for 15 min. A 10% RBC suspension was prepared using normal saline. The test solution, containing RBC suspension (0.5 ml), phosphate buffer pH 7.4 (1 ml, 0.15 M), hyposaline (2 ml, 0.36%), and various concentrations (10, 20, 40, 60, 80, and 100 mg/ml) of the sample solution, was prepared. Diclofenac sodium and isosaline were used to create standard and control solutions, respectively. The reaction mixtures were incubated at 37 °C for 30 min and then centrifuged at 3000 rpm for 20 min (15). Supernatant absorbance at 560 nm was measured using a UV-vis spectrophotometer (UV 1700, Shimadzu, Japan). The experiment was performed in triplicate, and RBC membrane stability (%) was calculated using the formula % stability = [100 - (ODsample/ODcontrol)] × 100.

GC-MS analysis of methanol fraction of *C. sinensis*

The bioactive methanol fraction of *C. sinensis*, identified as the most potent in preliminary investigations, underwent GC-MS analysis using an Agilent 8890 instrument. HP-5MS GC column (30 m × 250 µm × 0.25 µm) was employed. An Electron Impact Spectroscopy (EIS) detector with a fixed electron energy of 70 eV was utilized, while helium gas maintained a constant flow rate of 3 ml/min with a split ratio of 5:1. The sample injection volume was 1 µl. The oven temperature was programmed to increase at a rate of 5 °C/min up to 180 °C (hold time 3 min) and 300 °C (hold time 5 min), with a maximum set at 350 °C. The total run time was 53.5 min, including a 3.5 min solvent delay. Mass spectra within the range of 50-600 amu were scanned, and compound identification was performed by comparing the mass spectra with the NIST database (16).

In silico analysis

Pharmacokinetic analysis

Pharmacokinetic property analysis was conducted to assess the Absorption, Distribution, Metabolism, and Excretion (ADME) profiles of identified compounds through GC-MS. The ADME profiles, encompassing parameters such as drug-likeness based on Lipinski's Rule of Five, BBB permeability, Caco2 permeability, HIA percentage, skin permeability, as well as interactions with cytochrome P450 enzymes (2C19, 2C9, 2D6, and 3A4), were systematically evaluated for a total of 20 compounds. This comprehensive analysis was carried out utilizing SwissADME (http://www.swissadme.ch/) and PreADMET (https://preadmet.webservice.bmdrc.org/) platforms.

Toxicity profiling

Prior to *in silico* docking analysis, the toxicity profile of all GC-MS identified compounds (total no. 17) was evaluated for oral toxicity profiling by using ProTox-II (https://tox-new.charite.de/). The results were expressed as LD_{50} and toxicity class of the drug candidates (www. https://tox-new.charite.de/protox_II/).

Ligand preparation

The SDF files of GC-MS-identified compounds were retrieved from PubChem. The files were converted to .pdb file format in PyMOL (version 2.5.2). In the AutoDock tool (version 1.5.6), Gasteiger partial charges were added, merged nonpolar hydrogen atoms and torsional degrees of freedom were set in ligand, and the files were converted pdbqt file (17).

Receptor preparation

The X-ray crystal structures of secreted aspartic proteinase five from *C. albicans* (SAP5) (PDB ID: 2QZX), V-region of *Streptococcus mutans* antigen I/II (PDB ID: 1JMM), and C-terminal domain of *Streptococcus mutans* surface protein SpaP (PDB ID: 3OPU) were retrieved from protein data bank (PDB). All the parameters, such as removing water molecules, the addition of polar hydrogen atoms, heteroatoms (HETATM), Kollman charges, and preparation of the .pdbqt file of the receptors, were performed by using AutoDock (version 1.5.6) (17).

Molecular docking

Molecular docking analysis was conducted to assess the binding energies and affinities of seventeen ligands towards three distinct receptors (2QZX, 1JMM, and 3OPU) employing AutoDock Vina (version 1.5.6). The negative binding energy values, expressed in kilocalories per mole (kcal/mol), were utilized as indicators of binding affinity. The docking results were stored in the PDBQT format for subsequent analysis. Visualization and comprehensive examination of ligand-receptor interactions were performed using BIOVIA Discovery Studio Visualizer (version 2021) (17).

Results and Discussion

Antimicrobial study

The antimicrobial investigation was designed to assess the potential of *C. sinensis* in inhibiting pathogens while minimizing adverse effects on the host. Antimicrobial agents typically target processes such as cell wall synthesis, biochemical pathways, or microbial

biomolecules. The antibacterial efficacy of petroleum ether, chloroform, ethyl acetate, acetone, and methanol fractions derived from *C. sinensis* was evaluated against *Streptococcus mutans*, with corresponding zone of inhibition (ZOI) measurements of 10, 11, 18, 21, and 27 mm, respectively. In comparison, the standard drug gentamycin exhibited a ZOI of 29 mm (Fig. 1A). Given the superior bactericidal activity observed in the methanol fraction, its MIC and MBC were calculated as 0.78 and 1.56 mg/ml, respectively (Fig. 1B-C). These fractions were also subjected to antifungal testing against *Candida albicans*, revealing ZOI values of 9, 13, 19, 24, and 29 mm, respectively. In contrast, the standard drug amphotericin B exhibited a ZOI of 27 mm (Fig. 1A). Notably, the methanol fraction demonstrated the highest antifungal activity, with MIC and MFC recorded as 0.39 and 1.56 mg/ml, respectively (Fig. 1B-C). The antimicrobial efficacy of the methanol fraction of *C. sinensis* in this study can be attributed to the presence of bioactive compounds, including furaneol (18), glycerin (19), 5-hydroxymethylfurfural (20), 2-methoxy-4-vinylphenol (21), desulphosinigrin (22), 4',5,6,7,8-pentamethoxyflavone (23),

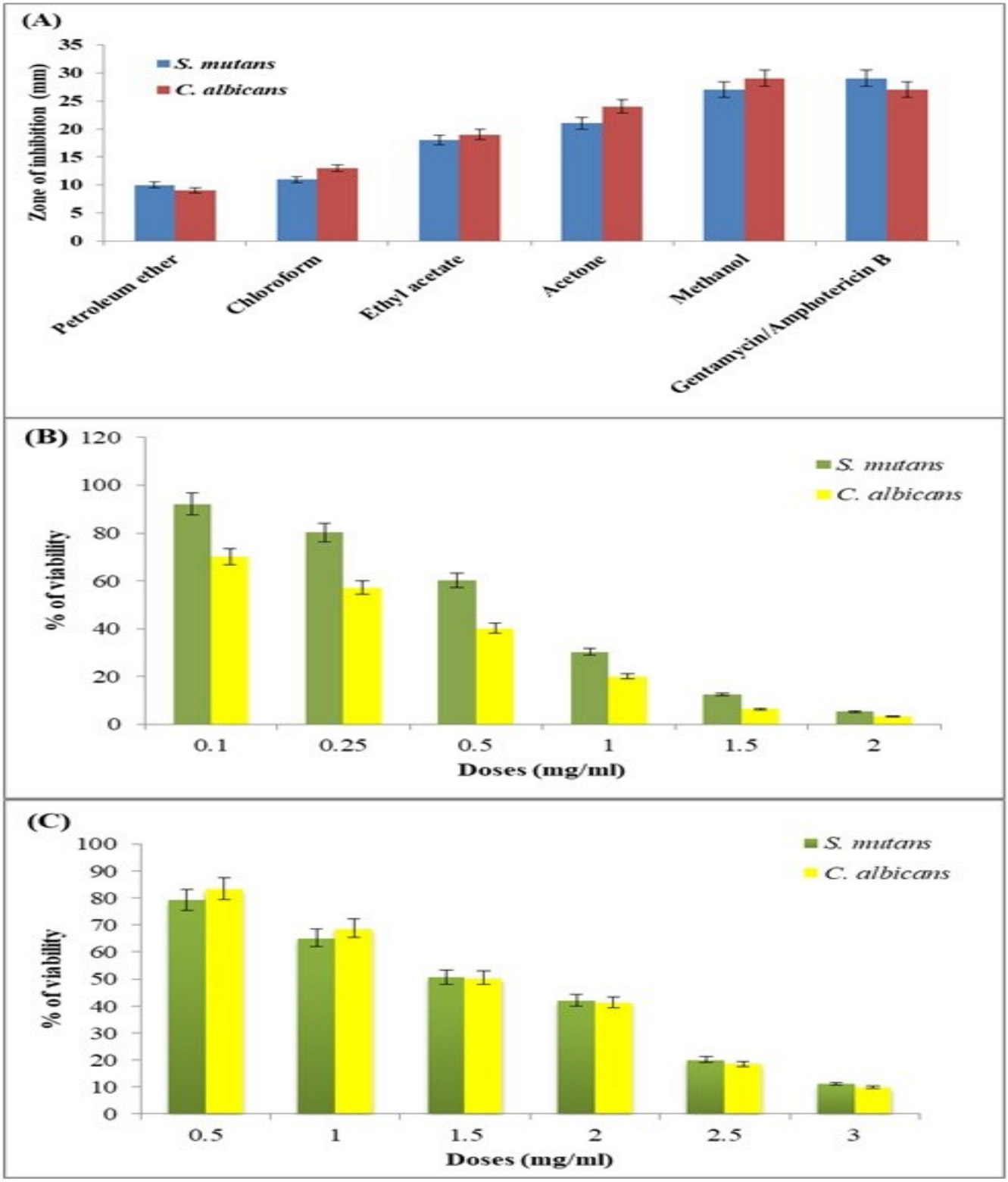

Figure 1. A. Represents zone of inhibition of different fractions of *C. sinensis*. B. Represents minimum inhibitory concentration of methanol fraction of *C. sinensis*. C. Represents minimum bactericidal/minimum fungicidal concentration of methanol fraction of *C. sinensis*

and 3',4',5,6,7,8-hexamethoxyflavone (24).

Ex-vivo anti-inflammatory assay

Dental caries is a persistent infectious ailment associated with inflammatory reactions in dental pulp (25). Odontoblasts, in response to this, generate chemokines and cytokines to modulate inflammatory processes (26). In light of the findings from the antimicrobial investigation, an *ex-vivo* assessment of the methanol fraction of *C.sinensis* was conducted to evaluate its anti-inflammatory activity. The methanol fraction demonstrated significant inhibition, reaching 79.26% at a concentration of 100 µg/ml, while the standard drug diclofenac sodium exhibited slightly higher inhibition at the same dosage, measuring 88.43% (Fig. 2). This observed effect is attributed to the presence of bioactive compounds such as glycerol (27), 4H -pyran-4-one, 2,3-dihydro-3,5-dihydroxy-6-methyl- (28), 5-hydroxymethylfurfural (29), and 2-methoxy-4-vinylphenol (30), including exo-2-hydroxycineole in the peel of *C.sinensis* (31).

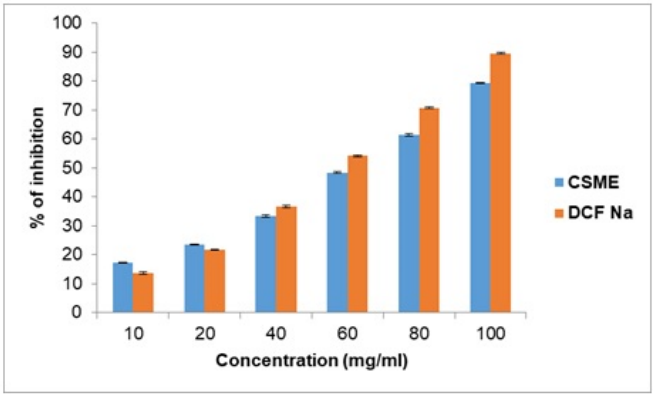

Figure 2. Represents *ex-vivo* anti-inflammatory activity of different concentrations of methanol fractions of *C. sinensis*. CSME: methanol fractions of *C. sinensis*, DCF Na (Diclofenac sodium): standard drug. Results were expressed as mean ± SD

GC-MS analysis of methanol fraction of *C. sinensis*

The methanol fraction exhibiting the highest bioactivity was subjected to GC-MS analysis to elucidate potential antimicrobial compounds within *C. sinensis.* A total of 17 compounds were identified, namely: 2,4-dihydroxy-2,5-dimethyl-3(2H)-furan-3-one (RT-4.363), 2H-pyran-2,6(3H)-dione (RT-4.6), 4-hydroxy-5-methyl-3(2H)-furanone (RT-5.484), furaneol (RT-5.725), glycerin (RT-6.695), 2,3-dihydro -3,5-dihydroxy-6-methyl-4H-pyran-4-one (RT-7.515), 5-hydroxymethylfurfural (RT-9.4), 2,3-dihydro-benzofuran (RT-9.098), 2-methoxy-4-vinylphenol (RT-11.431), 2,6-dimethyl-1,7-octadien-3-ol (RT-11.977), 1-methyl-4-(1-methylethenyl)-1,2-cyclohexanediol (RT-12.080), exo-2-hydroxycineole (RT-16.039), desulphosinigrin (RT-20.441), 5-O-desmethyltangeretin (RT-47.069), 4',5,6,7,8-pentamethoxyflavone (RT-47.417), 2-(3,4-dimethoxyphenyl) -5-hydroxy-6,7,8- trimethoxy-4H-chrom (RT-49.421), 3',4',5,6,7,8-hexamethoxyflavone (RT-49.859) (Table 1 and Fig. 3).

Lipinski's Rule of Five was employed for assessing the drug-likeness properties of compounds identified in the methanol fraction of *C. sinensis* (32). According to this rule, compounds violating two or more specific criteria are considered unsuitable for oral drug administration. All the compounds identified through GC-MS in the methanol fraction adhered to Lipinski's rule, meeting criteria such as molecular weight, hydrogen acceptors, hydrogen donors, clogP, and tPSA. Importantly, none of the compounds violated the Rule of Five, as detailed in Table 2. Pharmacokinetic properties, covering absorption,

Table 1. GC-MS profiling of methanol fraction of *C. sinensis*

Sl. no.	RT	Name of compound	Class	Molecular formula	Molecular mass
1	4.363	2,4-Dihydroxy-2,5-dimethyl-3(2H)-furan-3-one	Furan	$C_6H_8O_4$	144.13
2	4.600	2H-Pyran-2,6(3H)-dione	Pyran	$C_5H_4O_3$	112.08
3	5.484	3(2H)-Furanone, 4-hydroxy-5-methyl-	Furan	$C_7H_{10}O_3$	114.10
4	5.725	Furaneol	Furan	$C_6H_8O_3$	128.13
5	6.695	Glycerin	Alcohol	$C_3H_8O_3$	92.09
6	7.515	4H-Pyran-4-one, 2,3-dihydro-3,5-dihydroxy-6-methyl-	Pyran	$C_6H_8O_4$	144.13
7	9.400	5-Hydroxymethylfurfural	Furan	$C_6H_6O_3$	126.11
8	9.098	Benzofuran, 2,3-dihydro-	Benzofuran	$C_{15}H_{14}O$	120.15
9	11.431	2-Methoxy-4-vinylphenol	Phenol	$C_9H_{10}O_2$	150.17
10	11.977	1,7-Octadien-3-ol, 2,6-dimethyl-	Alcohol	$C_{10}H_{18}O$	154.25
11	12.080	1,2-Cyclohexanediol, 1-methyl-4-(1-methylethenyl)-	Alcohol	$C_{10}H_{18}O_2$	170.25
12	16.039	exo-2-Hydroxycineole	Monoterpenoid	$C_{10}H_{18}O_2$	170.25
13	20.441	Desulphosinigrin	Glucosinolate	$C_{10}H_{17}NO_6S$	279.31
14	47.069	5-O-Desmethyltangeretin	Flavone	$C_{19}H_{18}O_7$	360.36
15	47.417	4',5,6,7,8- Pentamethoxyflavone	Flavone	$C_{20}H_{20}O_7$	372.4
16	49.421	2-(3,4-Dimethoxyphenyl)-5-hydroxy-6,7,8- trimethoxy-4H-chrom	Flavone	$C_{20}H_{20}O_8$	390.38
17	49.859	3',4',5,6,7,8-Hexamethoxyflavone	Flavone	$C_{27}H_{32}O_{14}$	404.41

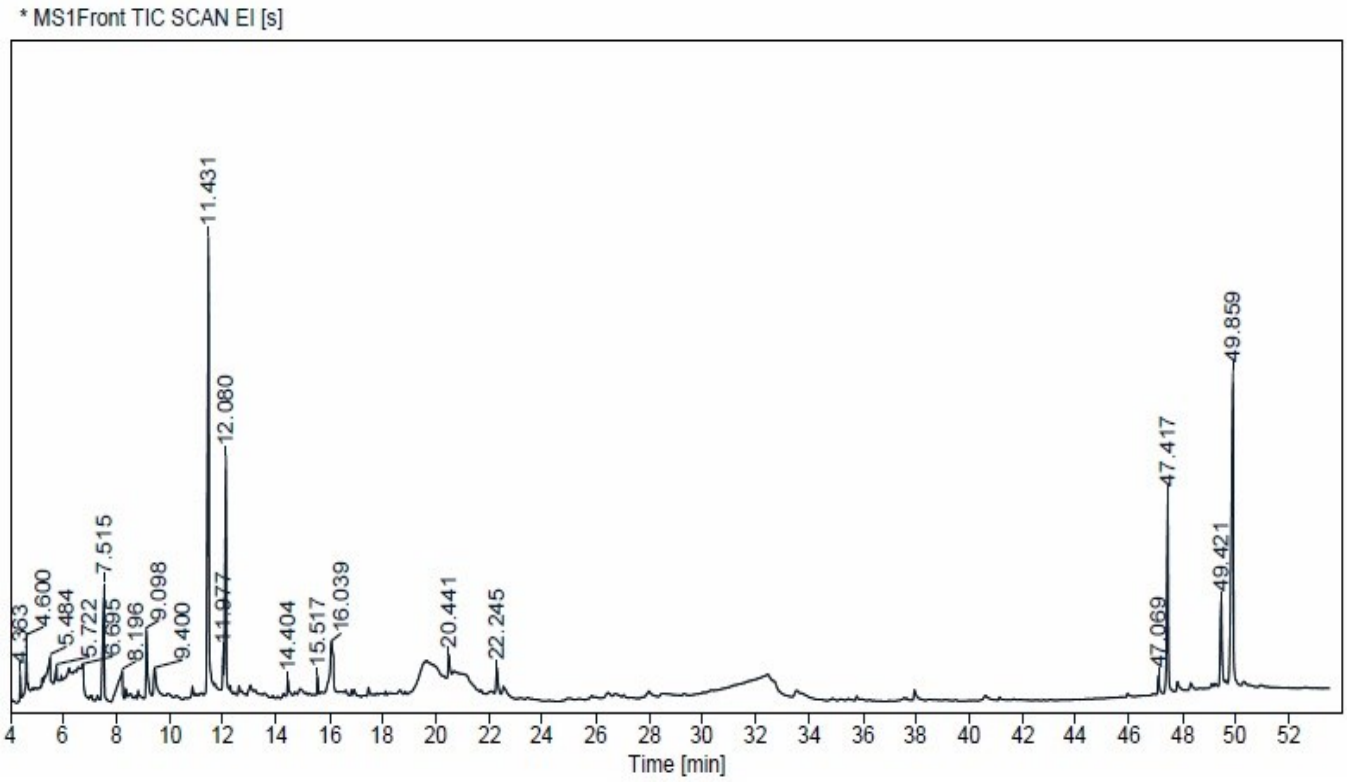

Figure 3. GC-MS spectrum of methanol fraction of *C. sinensis*

Table 2. Physiochemical parameters of GC-MS identified compounds

Sl. no.	Name	Lipinski rule of five (RO5)				
		Mol. wt	H-donor	H-acceptor	cLog P	tPSA
1	2,4-dihydroxy-2,5-dimethyl-3(2H)-furan-3-one	144.13	2	4	1.24	66.8
2	2H-pyran-2,6(3H)-dione	112.08	0	3	0.83	43.4
3	3(2H)-furanone, 4-hydroxy-5-methyl-	116.10	1	3	1.21	46.5
4	Furaneol	128.13	1	3	1.52	46.5
5	Glycerin	92.09	3	3	0.45	60.7
6	4H-pyran-4-one, 2,3-dihydro-3,5-dihydroxy-6- methyl-	144.13	2	4	1.19	66.8
7	5-hydroxymethylfurfural	126.11	1	3	0.91	50.44
8	Benzofuran, 2,3-dihydro-	120.15	0	1	1.89	9.2
9	2-methoxy-4-vinylphenol	150.17	1	2	2.14	29.5
10	1,7-octadien-3-ol, 2,6-dimethyl-	154.25	1	1	2.52	20.2
11	1,2-cyclohexanediol, 1-methyl-4-(1-methylethenyl)-	170.25	2	2	2.22	40.5
12	exo-2-hydroxycineole	170.25	1	2	2.29	29.5
13	Desulphosinigrin	279.31	5	7	0.85	148
14	5-O-desmethyltangeretin	360.36	1	7	3.38	83.45
15	4',5,6,7,8- pentamethoxyflavone	372.4	0	7	3.60	72.4
16	2-(3,4-dimethoxyphenyl)- 5-hydroxy-6,7,8-trimethoxy-4H-chrom	388.38	1	8	3.24	92.68
17	3',4',5,6,7,8-hexamethoxyflavone	404.41	0	8	3.76	81.68

distribution, metabolism, and excretion, are pivotal to a drug's pharmacodynamic characteristics (33). ADMET analysis of the 17 identified compounds revealed that 10 of them, including 2H-pyran-2,6(3H)-dione, N,N'-dibenzoyloxy heptanediamide, 2,3-dihydrobenzofuran, 2-methoxy-4-vinylphenol, 2,6-dimethyl-1,7-octadien-3-ol, exo-2-hydroxycineole, 5-O-desmethyltangeretin, 4',5,6,7,8-pentamethoxyflavone, 2-(3,4-dimethoxyphenyl)-5-hydroxy -6,7,8-trimethoxy-4H-chrom, and 3',4',5,6,7,8-hexamethoxyflavone, exhibited over 90% HIA. This suggests that upon oral administration, these compounds are likely to be absorbed to a significant extent. Additionally, LD_{50} values for all compounds, calculated using ProTox, ranged from 15 to 10000 mg/kg. Biotransformation, a critical aspect of drug efficacy, involves enzymatic processes, with cytochrome P450 (CYP450) being a key biotransforming enzyme (34). Among the 17 identified compounds, more than 50% acted as substrates for CYP450. Furthermore, most compounds demonstrated inhibitory effects on CYP2C19 and CYP2C9, as outlined in Table 3.

In silico analysis of selected compounds of methanol fraction of C. sinensis

The most potent bioactive methanol fraction of *C. sinensis* was shown to have effective antimicrobial activities against *S. mutans* and *C. albicans,* along with a significant anti-inflammatory response in the *ex-vivo* model. Based on their ADMET properties, to understand the inhibitory effects of 10 no. of GC-MS-identified bioactive compounds present in *C. sinensis* against *S. mutans* (PDB ID: 1JMM and 3OPU) and *C. albicans* (PDB ID: 2QZX), *in silico* molecular docking study was performed (35).

In the molecular docking studies, the compound 2H -pyran-2,6(3H)-dione manifested conventional hydrogen bonds with ARG824 and SER818, establishing robust interactions with 1JMM. Notably, a conventional hydrogen bond formed with ARG1193 in the case of 3OPU. Furthermore, it exhibited pronounced affinities for conventional hydrogen bonds with VAL330, TYR332, and GLY260 of 2QZX. The calculated binding affinities for this compound towards 1JMM, 3OPU, and 2QZX were determined as -5.0, -4.8, and -5.1 kcal/mol, respectively (Fig. 4A-C). Conversely, N,N'-di-benzoyloxy heptanediamide, upon docking with 1JMM, established conventional hydrogen bonds with SER704, LYS811, LYS812, and ASN814, accompanied by alkyl interaction

Table 3. PreADMET analysis of GC-MS identified compounds

Sl. No	Name of compounds	BBB	Caco2 permeability	HIA (%)	Skin permeability (logKpcm/h)	2C19 Inhibitor	2C9 Inhibitor	2D6 substrate	2D6 inhibitor	3A4 substrate	3A4 inhibitor	LD_{50} (mg/kg)	Toxicity class
1	2,4-dihydroxy-2,5-dimethyl-3(2H)-furanone	0.281557	2.9363	75.908308	-3.89462	non	yes	non	non	non	yes	1608	IV
2	2H-pyran-2,6(3H)-dione	0.809161	20.3111	90.750434	-2.81683	yes	yes	non	non	non	non	5000	V
3	3(2H)-furanone, 4-hydroxy-5-methyl-	0.330028	1.88683	87.577892	-4.4522	non	yes	non	non	non	yes	1932	IV
4	Furaneol	0.368044	1.10948	88.801551	-3.75576	non	yes	non	non	non	yes	1608	IV
5	Glycerin	0.179607	0.503894	63.518560	-4.0361	yes	yes	non	non	weakly	non	4090	V
6	4H-Pyran-4one, 2,3-dihydro-3,5-dihydroxy-6-methyl-	0.273964	1.85622	75.914677	-4.75733	non	yes	non	non	non	non	595	IV
7	5-hydroxymethylfurfural	0.52231	6.41666	88.682048	-2.9279	Yes	Yes	non	non	non	Yes	2500	V
8	Benzofuran, 2,3-dihydro-	1.20962	53.5016	100.000000	-1.91048	yes	yes	non	non	yes	non	1743	IV
9	2-methoxy-4-vinylphenol	1.47522	41.0619	96.736806	-1.43729	yes	yes	non	non	non	non	1560	IV
10	1,7-octadien-3-ol, 2,6-dimethyl-	6.43942	53.915	100.000000	-0.974645	Yes	yes	non	non	weakly	non	3900	V
11	1,2-cyclohexanediol, 1-methyl-4-(1-methylethenyl)-	2.39379	18.856	88.268092	-2.11195	non	yes	non	non	non	non	5000	V
12	exo-2-hydroxycineole	1.04569	34.5478	96.251160	-1.78856	non	yes	non	non	yes	yes	3080	V
13	Desulphosinigrin	0.082574	0.375984	31.323035	-4.96251	yes	yes	non	non	weakly	non	15	II
14	5-O-desmethyltangeretin	0.0144802	36.7898	96.576369	-3.56554	yes	yes	non	non	weakly	non	4000	V
15	4',5,6,7,8-pentamethoxyflavone	0.0414355	53.628	98.865394	-3.55725	yes	yes	non	non	yes	yes	5000	V
16	2-(3,4-dimethoxyphenyl)-5-hydroxy-6,7,8-trimethoxy-4H-chrom	0.0125793	41.2216	96.793753	-3.66449	yes	yes	non	non	weakly	yes	5000	V
17	3',4',5,6,7,8-hexamethoxyflavone	0.0203167	53.9372	98.023329	-3.25175	yes	yes	non	non	yes	yes	5000	V

with ILE815. Interaction with 3OPU resulted in the formation of a conventional hydrogen bond with TYR1421, ASN1408, and SER1444, alongside an aromatic ring forming π-alkyl interactions with VAL1410 and LYS1407. Interaction with 2QZX involved conventional hydrogen bonds with ASP218, GLY220, THR222, and ASP86, along with alkyl interactions with ILE305 and π-alkyl interactions with ALA119 and ILE30. The binding energies were recorded as -8.5 kcal/mol for 1JMM, and -9.3 kcal/mol for both 3OPU and 2QZX (Fig. 4D-F). Similarly, 2,3-dihydro-benzofuran displayed conventional hydrogen interactions with SER818 and LYS1438 of 1JMM and 3OPU, respectively, with binding energies of -5.1 and -4.7 kcal/mol, respectively. Additionally, it engaged in a conventional hydrogen interaction with SER88 of 2QZX, exhibiting a binding energy of -5.5 kcal/mol (Fig. 4G-I). Lastly, 2-methoxy-4-vinylphenol, when docked with 1JMM, formed conventional hydrogen interactions with GLU706 and π-alkyl interactions with PHE656 and TRP816, resulting in a binding energy of -5.3 kcal/mol. Interaction with 3OPU involved a conventional hydrogen bond with LYS1190 and ASN1227, and π-alkyl interactions with LYS1438, ALA1440, and TYR1421, yielding a binding energy of -5.2 kcal/mol. Notably, a stronger interaction was observed with 2QZX,

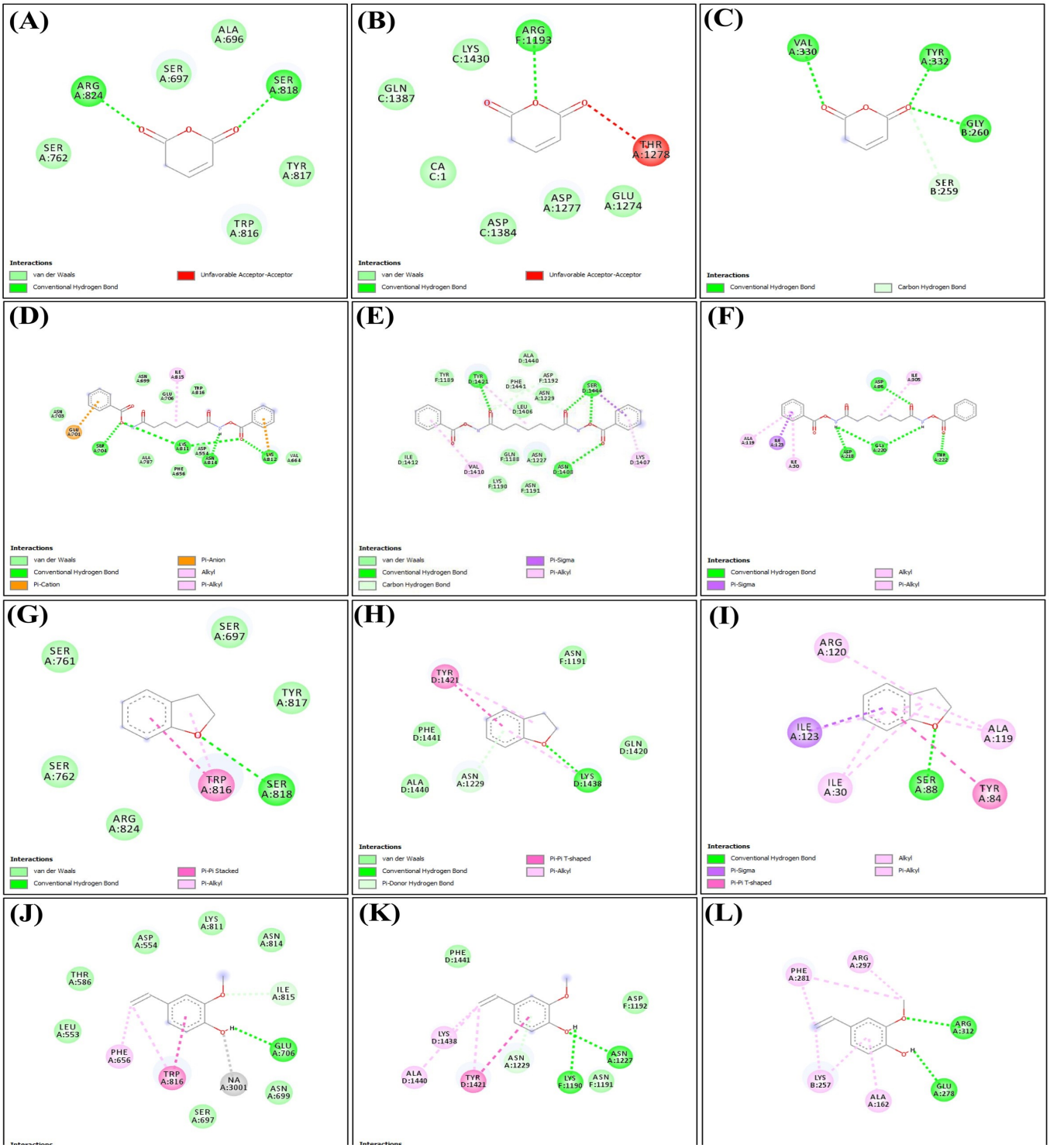

Figure 4. A-C. Represents docking of 2H-pyran-2,6(3H)-dione towards lJMM, 3OPU and 2QZX. D-F. Represents docking of N,N'-di-benzoyloxy heptanedia-mide towards lJMM, 3OPU and 2QZX. G-I. Represents docking of 2,3-dihydro-benzofuran towards lJMM, 3OPU and 2QZX. J-L. Represents docking of 2-methoxy-4-vinylphenol towards lJMM, 3OPU and 2QZX

involving conventional hydrogen bonds with GLU278 and ARG312, and π-alkyl interactions with ALA162, LYS257, PHE281, and ARG197, with a binding affinity of -5.7 kcal/mol (Fig. 4J-L).

2,6-dimethyl-1,7-octadien-3-ol exhibited a singular conventional hydrogen bond with GLU706, alongside π-alkyl interactions involving TRP816 and PHE656 in the of 1JMM. The calculated binding energy for this interaction was determined to be -4.8 kcal/mol. Within the framework of 3OPU, the compound engaged in a conventional hydrogen bond with PHE1441 and π-alkyl interactions with LYS1438, TYR1421, ALA1440, and LEU1406, resulting in a binding energy of -4.6 kcal/mol. Interaction with 2QZX was characterized by conventional hydrogen bonds formed with THR261, ASP263, and GLY205, complemented by a π-alkyl interaction with PRO329, yielding a binding energy of -5.0 kcal/mol (Fig. 5A-C). Exo-2-hydroxycineole, upon docking with 1JMM, formed a robust hydrogen bond solely with ASN814 and TRP816, resulting in a binding energy of -5.5 kcal/mol. Similarly, in the of 3OPU, a conventional hydrogen bond was established with ASN1191, yielding a binding energy of -5.7 kcal/mol. Interaction with 2QZX involved alkyl and π-alkyl bond formations with ILE30, ALA119, TYR84, and ILE123, accompanied by a reported binding energy of -5.7 kcal/mol (Fig. 5D-F). Furthermore, when docked with 1JMM, 5-O-desmethyltangeretin exhibited interactions with TRP816 and ARG824 exclusively through π-anion interactions, resulting in a remarkable binding affinity of -11.1 kcal/mol. In 3OPU docking, attractive forces with LYS1438 were

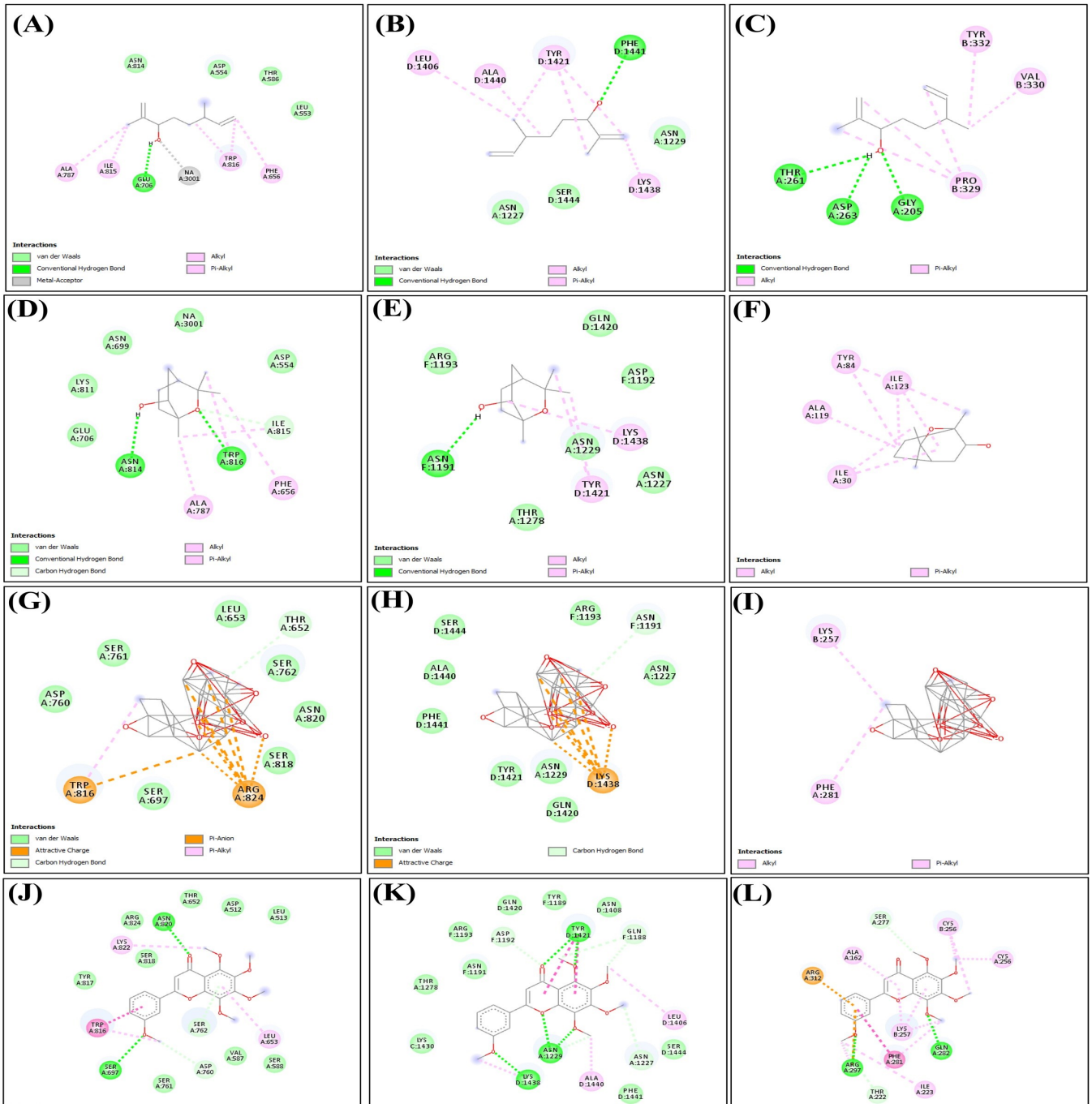

Figure 5. A-C. Represents docking of 2,6-dimethyl-l ,7-octadien-3-ol towards IJMM, 3OPU and 2QZX. D-F. represents docking of Exo-2-hydroxycineole towards JJMM, 3OPU and 2QZX. G-I. Represents docking of 5-O-desmethyltangeretin towards JJMM, 3OPU and 2QZX. J-L. Represents docking of 4',5,6,7,8- pentamethoxy flavone towards JJMM, 3OPU and 2QZX

identified, yielding a binding energy of -11.8 kcal/mol. Interaction with 2QZX involved alkyl interactions with LYS257 and PHE281, resulting in a binding affinity of -12.2 kcal/mol (Fig. 5G-I). In the case of 4',5,6,7,8-pentamethoxy flavone docking with 1JMM, conventional hydrogen interactions with SER697 and ASN820 were observed, alongside π-alkyl interactions involving LEU653 and TRP816, resulting in a binding energy of -7.7 kcal/mol. 3OPU docking revealed conventional hydrogen bonds with LYS1438, ASN1229, and TYR1421, with only TYR1421 participating in π-alkyl interactions. The binding energy for this interaction was determined to be -8.1 kcal/mol. Similarly, in 2QZX docking, conventional hydrogen interactions with ARG297 and GLN282, along with a π-alkyl interaction with PHE281, resulted in a binding affinity of -8.5 kcal/mol (Fig. 5J-L).

The compound 2-(3,4-dimethoxyphenyl)-5-hydroxy-6,7,8-trimethoxy-4H-chrom displayed conventional hydrogen interactions with ARG824 and π-alkyl interactions with TRP816 in the context of 1JMM, resulting in a binding energy of -7.4 kcal/mol. Conversely, during docking with 3OPU, it formed a sole conventional hydrogen bond with SER1444 and engaged in π-alkyl interaction with TYR1421, yielding a binding energy of -8.3 kcal/mol. When docked with 2QZX, the compound established three conventional hydrogen bonds with THR222, SER301, and ASP86, along with a π-alkyl interaction with ILE305, leading to a binding affinity of -7.8 kcal/mol (Fig. 6A-C). For 3',4',5,6,7,8-hexamethoxyflavone, docking with 1JMM showcased robust conventional hydrogen interactions with ASN820, ARG824, and SER818, as well as π-alkyl interactions with TRP816 and LEU653, resulting in a binding energy of -7.6 kcal/mol. In the of 3OPU, the compound exhibited only a single conventional hydrogen interaction with SER1444 and engaged in π-alkyl interaction with TYR1421, yielding a binding affinity of -7.5 kcal/mol. Docking with 2QZX revealed conventional hydrogen interaction with ARG312 and π-alkyl interaction with PHE281, resulting in a binding energy of -8.2 kcal/mol (Fig. 6D-F). Conversely, 7-oxo-2-oxa-7-thiatricyclo [4.4.0.0 (3,8)] decan-4-ol exhibited no discernible interactions with 1JMM, 3OPU, and 2QZX. The distinctive interaction profiles observed across these ligands with their respective receptors, coupled with the calculated binding energies, suggest a potential basis for their significant antimicrobial activity, likely attributed to the diverse functional groups present in the ligands.

Conclusion

The ongoing investigation has unveiled the robust bioactive properties of the methanol fraction extracted from the peel of Citrus sinensis. This fraction exhibits significant *in vitro* antimicrobial efficacy and *ex-vivo* anti-inflammatory potential against dental caries. Through GC-MS analysis, various bioactive compounds were identified, demonstrating notable activity against dental caries pathogens, including *Streptococcus mutans* and *Candida albicans*. Moreover, the research is substantiated by pharmacokinetic analysis and in silico docking studies focusing on selected compounds identified through GC-MS. Notably, among the ten compounds scrutinized, 5-O-*demethyltangeretin* and N,N'-di-benzoyloxy heptanediamide emerged as the most prominent interactors with the defined receptors of *S. mutans* and

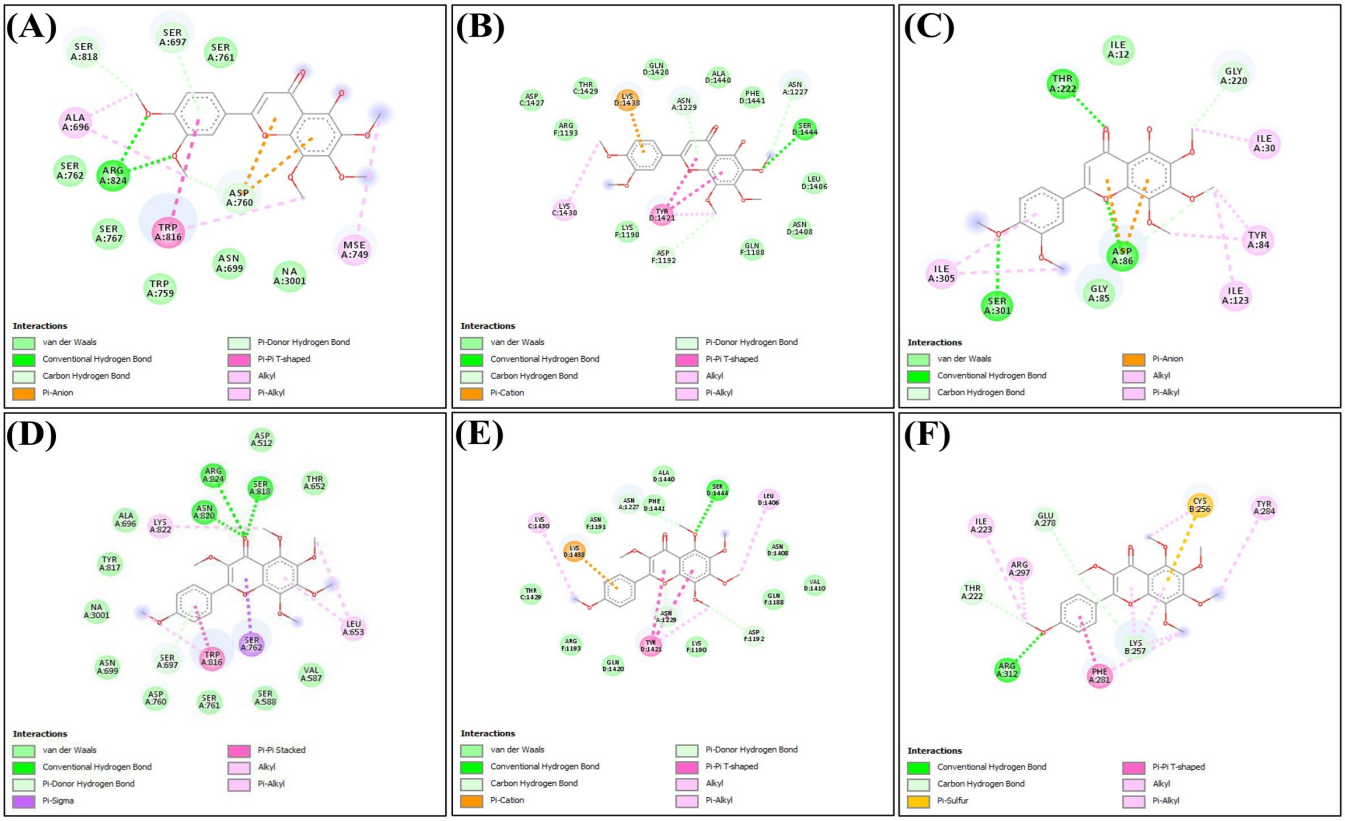

Figure 6. A-C. Represents docking of 2-(3,4-dimethoxyphenyl)-5-hydroxy-6 ,7,8-trimethoxy-4H-chrom towards IJMM, 3OPU and 2QZX. D-F. Represents docking of 3',4',5,6,7,8-hexamethoxyflavone towards IJMM, 3OPU and 2QZX

C. albicans, as revealed by *in silico* studies. Considering the current findings and supporting evidence, future research avenues may encompass the isolation of these bioactive compounds, *in vivo* studies, and an exploration of the molecular mechanisms underlying the effects of the methanol fraction or its potent bioactive constituents from Citrus sinensis.

Acknowledgements

The authors are thankful to Centurion University of Technology and Management, Odisha, IMS & Sum Hospital Medical College, Siksha O Anusandhan University, Odisha, and SAIF, IIT-Madras, for providing an instrumental facility.

Authors' contributions

Satyaprakash Dehury: Investigation. Priyanka Priyadarsini: Investigation. Ashirbad Nanda: Investigation, writing, review, and editing. Debasmita Dubey: Investigation. Sandeep Kumar Swain: Formal analysis. Biswajit Samantaray: Resources. Barsha Tripathy: Sample collection. Satish Kanhar: Conceptualization, methodology, investigation, writing-original draft, editing, and formal analysis.

Compliance with ethical standards

Declaration : Authors do not have any conflict of interest to declare.

Ethical issues: None.

References

1. M. Global burden of bacterial antimicrobial resistance in 2019: A systematic analysis. Lancet. 2022;399:629-55. https://doi.org/10.1016/S0140-6736(21)02724-0.
2. Chen X, Daliri EB, Kim N, Kim J, Yoo D, Oh D. Microbial etiology and prevention of dental caries: Exploiting natural products to inhibit cariogenic biofilms. Pathogens. 2020;9:1-15. DOI: 10.3390/pathogens9070569.
3. Karoly M, Gabor N, Adam N, Andrea B. Characteristics, diagnosis and treatment of the most common bacterial diseases of the oral cavity. Orvosi Hetilap. 2019;160:739-46. DOI: 10.1556/650.2019.31377.
4. Yadav K, Prakash S. Dental caries: A microbiological approach. J Clin Infect Dis Pract. 2017;2:1-15. DOI: 10.4172/2476-213X.1000118
5. Milind P, Chaturvede D. Orange: Range of benefits. Int Res J Pharm. 2012;3:59-63.
6. Kaviya S, Santhanalakshmi J, Viswanathan B, Muthumary J, Srinivasan K. Biosynthesis of silver nanoparticles using *Citrus sinensis* peel extract and its antibacterial activity. Spectrochim Acta A Mol Biomol Spectrosc. 2011;79:594-98. DOI: 10.1016/j.saa.2011.03.040.
7. Naila A, Nadia D, Zahoor QS. Stable silver nanoparticles synthesis by *Citrus sinensis* (orange) and assessing activity against food poisoning microbes. Biomed Environ Sci. 2014;27:815-18. DOI: 10.3967/bes2014.118.
8. Trovato A, Monforte MT, Forestieri AM, Pizzimenti F. *In vitro* anti-mycotic activity of some medicinal plants containing flavonoids. Boll Chim Farm. 2000;139:225-27.
9. Bagavan A, Rahuman AA, Kamaraj C, Kaushik NK, Mohanakrishnan D, Sahal D. Antiplasmodial activity of botanical extracts against *Plasmodium falciparum*. Parasitol Res. 2011;108:1099-109. DOI: 10.1007/s00436-010-2151-0.
10. Favela-Hernández JMJ, González-Santiago O, Ramírez-Cabrera MA, Patricia C, Esquivel-Ferriño PC, Camacho-Corona MR. Chemistry and pharmacology of *Citrus sinensis*. Molecules. 2016;21:1-24. DOI: 10.3390/molecules21020247.
11. Yucra S, Gasco M, Rubio J, Nieto J, Gonzales GF. Effect of different fractions from hydroalcoholic extract of Black Maca (*Lepidium meyenii*) on testicular function in adult male rats. Fertil Steril. 2007;89:1461-67. DOI: 10.1016/j.fertnstert.2007.04.052.
12. Dubey D, Padhy RN. Antibacterial activity of *Lantana camara* L. against multidrug resistant pathogens from ICU patients of a teaching hospital. J Herb Med. 2013;3:65-75. https://doi.org/10.1016/j.hermed.2012.12.002.
13. Abiola C, Oyetayo VO. Isolation and biochemical characterization of microorganisms associated with the fermentation of Kersting's groundnut (*Macrotyloma geocarpum*). Res J Microbiol. 2016;11:47-55. https://doi.org/10.3923/jm.2016.47.55
14. Bishoyi AK, Mahapatra M, Sahoo CR, Paidesetty SK, Padhy RN. Design, molecular docking and antimicrobial assessment of newly synthesized p-cuminal-sulfonamide Schiff base derivatives. J Mol Struct. 2021;1250:1-14. https://doi.org/10.1016/j.molstruc.2021.131824.
15. Sajid-ur-Rehman M, Ishtiaq S, Khan MA, Alshamrani M, Younus M, Shaheen G *et al*. Phytochemical profiling, *in vitro* and *in vivo* anti-inflammatory, analgesic and antipyretic potential of *Sesuvium sesuvioides* (Fenzl) Verdc. (Aizoaceae). Inflammopharmacology. 2021;29:789-800. DOI: 10.1007/s10787-021-00824-9.
16. Kanhar S, Sahoo AK. Ameliorative effect of *Homalium zeylanicum* against carbon tetrachloride induced oxidative stress and liver injury in rats. Biomed Pharmacother. 2019;111:305-14. https://doi.org/10.1016/j.biopha.2018.12.045.
17. Siddique MH, Andleeb R, Ashraf A, Zubair M, Fakhar-e-Alam M, Hayat S *et al*. Integration of *in silico* and *in vitro* approaches to evaluate antioxidant and anticancer properties of *Tribulus terrestris* extracts. Arab J Chem. 2022;15:1-12. https://doi.org/10.1016/j.arabjc.2022.103984.
18. Schwab W. Natural 4-hydroxy-2,5-dimethyl-3(2H)-furanone (Furaneol®). Molecules. 2013 13;18(6):6936-51. DOI: 10.3390/molecules18066936.
19. Nalawade TM, Bhat K, Sogi SHP. Bactericidal activity of propylene glycol, glycerine, polyethylene glycol 400 and polyethylene glycol 1000 against selected microorganisms. J Int Soc Prev Community Dent. 2015;5:114-19. DOI: 10.4103/2231-0762.155736.
20. Duru CE, Duru IA, Nwagbara NK. Potency of 5-hydroxymethylfurfuraldehyde (HMF) against *Bacillus cereus* and *Proteus mirabilis*. Biochem Indian J. 2012;6:41-44.
21. Rubab M, Chelliah R, Saravanakumar K, Barathikannan K, Wei S, Kim J, Yoo D *et al*. Bioactive potential of 2-methoxy-4-vinylphenol and benzofuran from *Brassica oleracea* L. var. *capitate* f, *rubra* (red cabbage) on oxidative and microbiological stability of beef meat. Foods. 2020;9:1-22. DOI: 10.3390/foods9050568.
22. Olajuyigbe OO, Onibudo TE, Coopoosamy RM, Ashafa AOT, Afolayan AJ. Bioactive compounds and *in vitro* antimicrobial activities of ethanol stem bark extract of *Trilepisium madagascariense* DC. Int J Pharmacol. 2018;14:901-12. DOI: 10.3923/ijp.2018.901.912.
23. Shamsudin NF, Ahmed QU, Mahmood S, Shah SAA, Khatib A,

Mukhtar S *et al*. Antibacterial effects of flavonoids and their structure-activity relationship study: A comparative interpretation. Molecules. 2022;27:1-43. https://doi.org/10.3390/molecules27041149.

24. Johann S, Oliveira VLD, Pizzolatti MG, Schripsema J, Braz-Filho R, Branco A *et al*. Antimicrobial activity of wax and hexane extracts from *Citrus* spp. peels. Mem Inst Oswaldo Cruz. 2007;102:681-85. DOI: 10.1590/s0074-02762007005000087.
25. Farges J, Alliot-Licht B, Renard E, Ducret M, Gaudin A, Smith AJ *et al*. Dental pulp defence and repair mechanisms in dental caries. Mediators Inflamm. 2015;2015:1-16. DOI: 10.1155/2015/230251.
26. Galler KM, Weber M, Korkmaz Y, Widbiller M, Feuerer M. Inflammatory response mechanisms of the dentine-pulp complex and the periapical tissues. Int J Mol Sci. 2021;22:1-23. DOI: 10.3390/ijms22031480.
27. Szél E, Polyánka H, Szabó K, Hartmann P, Degovics D, Balázs B *et al*. Anti-irritant and anti-inflammatory effects of glycerol and xylitol in sodium lauryl sulphate-induced acute irritation. J Eur Acad Dermatol Venereol. 2015;29:2333-41. DOI: 10.1111/jdv.13225.
28. Sharma N, Samarakoon KW, Gyawali R, Park Y, Lee S, Oh SJ *et al*. Evaluation of the antioxidant, anti-Inflammatory and anticancer activities of *Euphorbia hirta* ethanolic extract. Molecules. 2014;19:14567-81. DOI: 10.3390/molecules190914567.
29. Kong F, Lee BH, Wei K. 5-hydroxymethylfurfural mitigates lipopolysaccharide-stimulated inflammation via suppression of MAPK, NF-κB and mTOR activation in RAW 264.7 cells. Molecules. 2019;13:1-16. DOI: 10.3390/molecules24020275.
30. Jeong JB, Hong SC, Jeong HJ, Koo JS. Anti-inflammatory effect of 2-methoxy-4-vinylphenol via the suppression of NF-κB and MAPK activation, and acetylation of histone H_3. Arch Pharm Res. 2011;34:2109-16. DOI: 10.1007/s12272-011-1214-9.
31. Shabbir A, Batool SA, Bashee MI, Shahzad M, Sultana K, Tareen RB *et al*. *Ziziphora clinopodioides* ameliorated rheumatoid arthritis and inflammatory paw edema in different models of acute and chronic inflammation. Biomed Pharmacother. 2018;97:1710-21. DOI: 10.1016/j.biopha.2017.11.118.
32. Lipinski CA, Lombardo F, Dominy BW, Feeney PJ. Experimental and computational approaches to estimate solubility and permeability in drug discovery and development settings. Adv Drug Deliv Rev. 1997;23:3-25. DOI: 10.1016/s0169-409x(00)00129-0.
33. Srivastava V, Yadav A, Sarkar P. Molecular docking and ADMET study of bioactive compounds of *Glycyrrhiza glabra* against main protease of SARS-CoV2. Materials Today: Proceedings. 2022;49:2999-3007. DOI: 10.1016/j.matpr.2020.10.055.
34. Nisha CM, Kumar A, Nair P, Gupta N, Silakari C, Tripathi T *et al*. Molecular docking and *in silico* ADMET study reveals acylguanidine 7a as a potential inhibitor of β-secretase. Adv Bioinform. 2016;2016:1-7. DOI: 10.1155/2016/9258578.
35. Mandujano-Gonzáleza V, Villa-Tanaca L, Anducho-Reyes MA, Mercado-Flores Y. Secreted fungal aspartic proteases: A review. Revista Iberoamericana de Micología. 2016;33:76-82. https://doi.org/10.1016/j.riam.2015.10.003.